ACS OMEGA

http://pubs.acs.org/journal/acsodf

Article

Mitochondrial Imbalance of *Trypanosoma cruzi* Induced by the Marine Alkaloid 6-Bromo-2′-de-*N*-Methylaplysinopsin

Maiara M. Romanelli, Maiara Amaral, Fernanda Thevenard, Lucas M. Santa Cruz, Luis O. Regasini, Alvaro E. Migotto, João Henrique G. Lago,* and Andre G. Tempone*

Cite This: *ACS Omega* 2022, 7, 28561−28570

Read Online

ACCESS | Metrics & More | Article Recommendations | Supporting Information

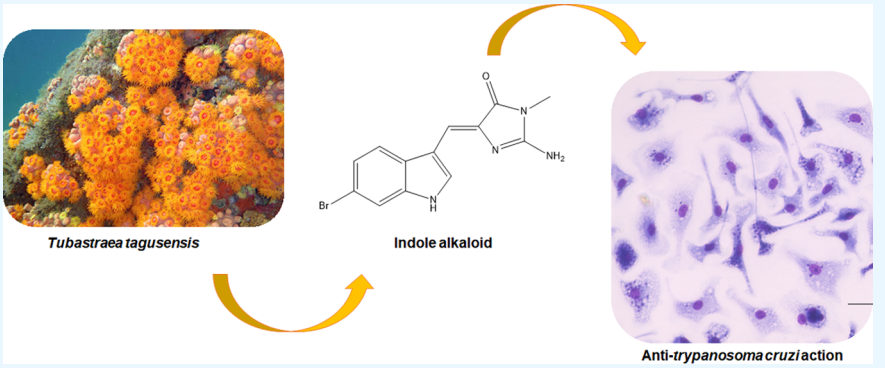

ABSTRACT: Chagas disease, caused by *Trypanosoma cruzi*, affects seven million people worldwide and lacks effective treatments. Using bioactivity-guided fractionation, NMR, and electrospray ionization-high resolution mass spectrometry (ESI-HRMS) spectral analysis, the indole alkaloid 6-bromo-2′-de-*N*-methylaplysinopsin (**BMA**) was isolated and chemically characterized from the marine coral *Tubastraea tagusensis*. **BMA** was tested against trypomastigotes and intracellular amastigotes of *T. cruzi*, resulting in IC_{50} values of 62 and 5.7 μM, respectively, with no mammalian cytotoxicity. The mechanism of action studies showed that **BMA** induced no alterations in the plasma membrane permeability but caused depolarization of the mitochondrial membrane potential, reducing ATP levels. Intracellular calcium levels were also reduced after the treatment, which was associated with pH alteration of acidocalcisomes. Using matrix-assisted laser desorption/ionization-time of flight (MALDI-TOF)/MS analysis, alterations of mass spectral signals were observed after treatment with **BMA**, suggesting a different mechanism from benznidazole. In silico pharmacokinetic−pharmacodynamic (PKPD) parameters suggested a drug-likeness property, supporting the promising usefulness of this compound as a new hit for optimizations.

1. INTRODUCTION

Chagas disease is a neglected parasitic infection caused by *Trypanosoma cruzi*. In Latin America and southern parts of the United States of America, it has affected approximately seven million people, with 70 million at risk of infection.[1] Migratory population movements have contributed to the spread of the disease, resulting in an emergent worldwide public health issue.[2]

T. cruzi infects humans during the blood meal of triatomine bugs through the contact of the bite site with insect feces.[1,3] The disease has an acute phase with peaks of parasitemia, but most symptoms are absent or mild. A chronic phase is stabilized when most parasites are inside the heart cells, causing cardiomyopathy, and in digestive muscles, resulting in the megacolon and megaesophagus in 30% of patients. Additionally, chronic stages can also cause a neurological disorder and death caused by heart failure.[4,5] Considering the elevated numbers of COVID-19 infections around the world, the prognosis of Chagas disease (CD) patients could be highly impacted. Recently, infections caused by SARS-CoV-2 (COVID-19) have also been shown to affect the cardiovascular system,[6] increasing the difficulties related to the clinical treatment of CD patients.

Currently available drugs are two highly toxic nitro-compounds, nifurtimox and benznidazole. Both have decreased effectiveness in the chronic phase. Moreover, both drugs require prolonged treatment with severe side effects, resulting in different treatment success according to the parasite strain.[7] In Brazil, benznidazole is the only available drug with an

Received: May 31, 2022
Accepted: July 27, 2022
Published: August 4, 2022

efficacy of 70% during the acute phase and 10−20% during the chronic phase.[2,8,9] The toxicity and poor efficacy of the current treatment show the critical situation for CD and demonstrate the urgency for new drugs.

Natural products from plants, microorganisms, and marine invertebrates have served as an inspiration for the design of several FDA-approved drugs. Between 1981 and 2019, drugs and synthetic molecules based on natural products accounted for over 50% of new drugs.[10] Among the approved marine-derived drugs, it is possible to include anticancer drugs, antivirals, and drugs to treat neuropathic pain and hypertriglyceridemia.[11−15]

Tubastraea tagusensis is a coral (Order Scleractinia) that produces a calcium skeleton for protection against other animals. The invasion of these azooxantellate corals started in the Campos Basin in Brazil in the 1980s. Currently, these corals are spread over more than 3,500 km of the Brazilian coast.[16] *Tubastraea* spp. are a risk to local organisms and are considered an invasive species. The production of toxins contributes to this defense against predation by fish and other organisms, usually competing for space and substrates.[17] These chemical compounds have considerable pharmacological activities and include polyoxazole macrolides, anthraquinone derivatives, fatty acid sterols, and alkaloids.[17−20]

In this work, the activity of the MeOH extract of *T. tagusensis* was investigated against *T. cruzi*. Using bioactivity-guided fractionation, the active compound was isolated and chemically characterized by nuclear magnetic resonance (NMR) and high-resolution electrospray ionization mass spectrometry (ESI-HRMS) spectral analysis. The in vitro potency, mammalian cytotoxicity, and lethal mechanisms against the parasite were also investigated. Additionally, the physicochemical properties and pharmacokinetic−pharmacodynamic (PKPD) parameters were evaluated using an in silico-based approach.

2. RESULTS

2.1. Chemical Characterization. NMR (^{1}H and ^{13}C) and ESI-HRMS data (see the Supporting Information) of the bioactive compound from *T. tagusensis* (purity of 99% by high-performance liquid chromatography (HPLC)) were compared with the literature,[21,22] allowing for the identification of 6-bromo-2′-de-*N*-methylaplysinopsin (**BMA**, Figure 1). Additionally, the stereochemistry of double bond at C-8/C-1′ was determined as (*E*)- by the comparison of ^{13}C NMR data of both diastereomers previously reported in the literature.[23]

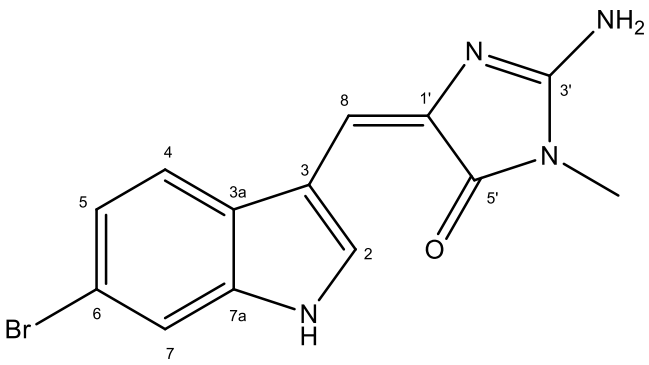

Figure 1. Chemical structure of 6-bromo-2′-de-*N*-methylaplysinopsin (**BMA**) isolated from *T. tagusensis*.

2.2. Antitrypanosomal Activity. To select bioactive compounds, the bioactivity-guided fractionation of the MeOH extract of *T. tagusensis* was performed. Initially, the crude MeOH extract was partitioned using *n*-hexane, EtOAc, and *n*-butanol and afforded a bioactive EtOAc phase. This phase was chromatographed on a Sephadex LH-20 to afford six groups (A−F) with bioactivity concentrated on fraction E. This fraction was purified by HPLC to afford 6-bromo-2′-de-*N*-methylaplysinopsin (**BMA**, Table 1). To conduct antitrypanosomal assays, trypomastigotes were incubated (150 μg/mL) for 24 h, and the morphology was examined using microscopy.

Table 1. Antitrypanosomal Activity of the Crude MeOH Extract, Partition Phases, and Fractions of the Coral *T. tagusensis*

tested material	% death of trypomastigotes at 150 μg/mL
MeOH extract	0
n-butanol phase	0
EtOAc phase	100
n-hexane phase	0
fraction A*	0
fraction B*	0
fraction C*	0
fraction D*	0
fraction E*	100
fraction F*	0

*Fractions A−F are pooled fractions of the EtOAc extract applied to a Sephadex LH-20 column.

BMA was tested in trypomastigotes and intracellular amastigotes and presented IC_{50} values of 62 and 5.7 μM, respectively. Benznidazole resulted in IC_{50} values of 16.2 and 5.3 μM against trypomastigotes and intracellular amastigotes, respectively. Mammalian cytotoxicity was analyzed with NCTC clone 929 cells using the MTT method. The results indicated no toxicity at the highest tested concentration of 200 μM (Table 2).

Table 2. Evaluation of the 50% Inhibitory Concentration (IC_{50}) of BMA and the Positive Control Benznidazole against *T. cruzi* and Cytotoxicity (CC_{50})[a]

compound	IC_{50} ± SD (μM) trypomastigotes	IC_{50} ± SD (μM) amastigotes	CC_{50} ± SD (μM)	SI
BMA	62.7 ± 8.1	5.7 ± 2.2	>200	>34.5
benznidazole	16.2 ± 3.7	5.3 ± 0.3	>200	>38.4

[a]CC_{50}: 50% cytotoxic concentration in NCTC cells; IC_{50}: 50% inhibitory concentration in trypomastigotes and intracellular amastigotes; selectivity index (SI), given by the ratio between CC_{50} and IC_{50} (amastigote); standard deviation (SD).

2.3. In Silico ADME/Physicochemical Analysis. Considering the activity against *T. cruzi*, **BMA** was evaluated in silico, according to the chemical structure, using the SwissADME platform. The analysis was performed to investigate safety, pharmacokinetic/pharmacodynamic properties, and the drug-likeness profile. The ADMET properties are presented in Table 3.

BMA presented a molecular weight of 319 g/mol with a Log *P* of 1.7 and moderate water solubility. The pharmacoki-

https://doi.org/10.1021/acsomega.2c03395
ACS Omega 2022, 7, 28561−28570

Table 3. In Silico Physicochemical and ADMET Parameters of 6-Bromo-2′-de-*N*-methylaplysinopsin (BMA)[a]

parameters	BMA
fraction of carbons sp^3	0.08
no. of rotatable bonds	1
no. of H-bond acceptors	2
no. of H-bond donors	2
TPSA (Å^2)	74.48
Log *P*	1.73
Log *S*	−3.21
gastrointestinal absorption	high
permeability in the blood−brain barrier	×
P-gp substrate	×
inhibitor CYP1A2	√
inhibitor CYP2C19	√
inhibitor CYP2C9	×
inhibitor CYP2D6	×
inhibitor CYP3A4	×
Lipinski	√
Ghose	√
Veber	√
Egan	√
Muegge	√
Leadlikness	√

[a]CYP: cytochrome P450; P-gp: *P*-glycoprotein; TPSA: topological polar surface area; √, Yes; ×, No.

netic parameters predicted high gastrointestinal absorption with no permeation into the blood−brain barrier. **BMA** showed that it was not prone to act as a substrate for *P*-glycoprotein but can act as a possible inhibitor of two major cytochrome P450 enzymes (CYP1A2 and CYP2C9). **BMA** passed in all drug-likeness filters (Lipinski, Ghose, Egan, and Muegge) with no violations.

2.4. Mechanism of Action (MoA) Studies. Trypomastigotes were treated with **BMA** for up to 4 h to define the best time and concentration for the mechanism of action (MoA) assays. After 2 h of treatment, IC_{50} was defined as 130 μM. Therefore, all MoA studies were carried out under these conditions.

2.5. Effects of BMA on the Plasma Membrane. Sytox Green was utilized to measure damages to the plasma membrane integrity of trypomastigotes. The treatment with **BMA** (at 130 μM) showed no alteration in plasma membrane permeability, with fluorescence levels similar to those of untreated parasites after 2 h of incubation (Figure 2). Triton X-100 was employed as an internal control ($p < 0.001$).

2.6. Effects of BMA on the Mitochondrial Potential ($\Delta\Psi_m$). Changes in the $\Delta\Psi_m$ of trypomastigotes were verified by the JC-1 probe. When compared to untreated parasites (1 and 2 h), significant depolarization of the parasite membrane was observed ($p < 0.01$). CCCP was used as a positive control and the untreated parasites were used as a negative control (Figure 3).

2.7. Measurement of ATP Levels. The ATP determination kit was used to quantify ATP in trypomastigotes. The treatment with **BMA** (130 μM) resulted in a significant decrease in the ATP concentration ($p < 0.001$) after 2 h of treatment when compared to untreated parasites. The control CCCP (100 μM), an oxidative phosphorylation uncoupler, was used for the maximum reduction in the ATP levels (Figure 4).

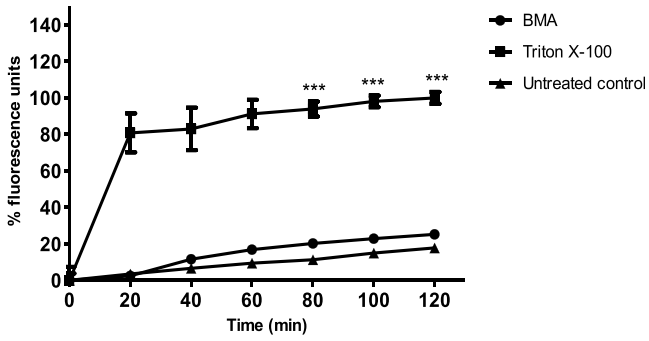

Figure 2. Evaluation of plasma membrane permeability in trypomastigotes of *T. cruzi* after 2 h of treatment with **BMA** using the Sytox Green probe (485 nm excitation and 535 nm emission). Untreated and 0.5% Triton X-100-treated parasites were used as negative and positive controls, respectively. Fluorescence is reported as a percentage relative to the positive control (Triton X-100) at 120 min (100% permeabilization). ***$p < 0.001$ relative to the negative control.

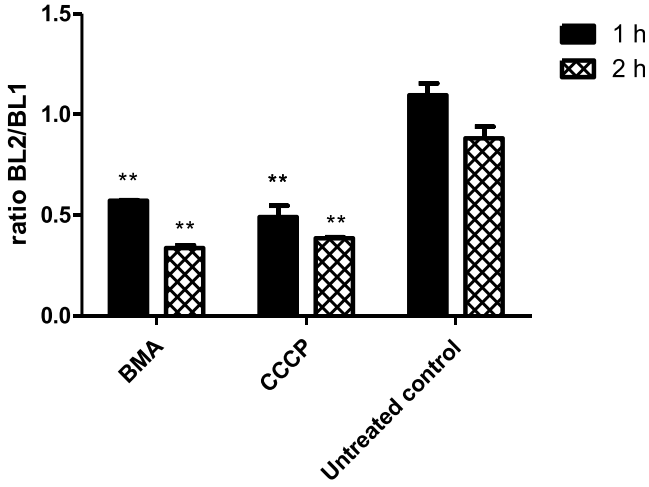

Figure 3. Evaluation of the mitochondrial potential in trypomastigotes after 1 and 2 h of treatment with **BMA** using the JC-1 probe (488 nm excitation and 530/574 nm emission). CCCP was used as a positive control and the untreated parasites as a negative control. Data are reported as the ratio of 574 and 530 nm. **$p < 0.01$ relative to the negative control.

2.8. Measurement of Reactive Oxygen Species (ROS). The analysis of ROS was carried out using the H_2DCFDA dye. **BMA** (130 μM) did not alter the ROS levels when compared to untreated parasites at 1 and 2 h of incubation. Sodium azide (10 mM) was used as a positive control (Figure 5).

2.9. Calcium (Ca^{2+}) Evaluation. Cytosolic calcium was measured in trypomastigotes using the Fluo-4 AM dye. According to the data presented in Figure 6, the treatment with **BMA** (130 μM) did not alter intracellular calcium levels when compared to the untreated control. Ca^{2+} upregulation was observed with Triton X-100 (control).

2.10. Acidocalcisomes. Alterations in the acidocalcisomes of trypomastigotes were evaluated using the acridine orange dye. **BMA** induced a reduction in the fluorescence after 1 h of incubation, as a result of pH alteration of the acidocalcisomes. After this period, the pH reverted to the basal levels observed in the untreated parasites. Nigericin increased the fluorescence after a rapid incubation period (Figure 7).

https://doi.org/10.1021/acsomega.2c03395
ACS Omega 2022, 7, 28561−28570

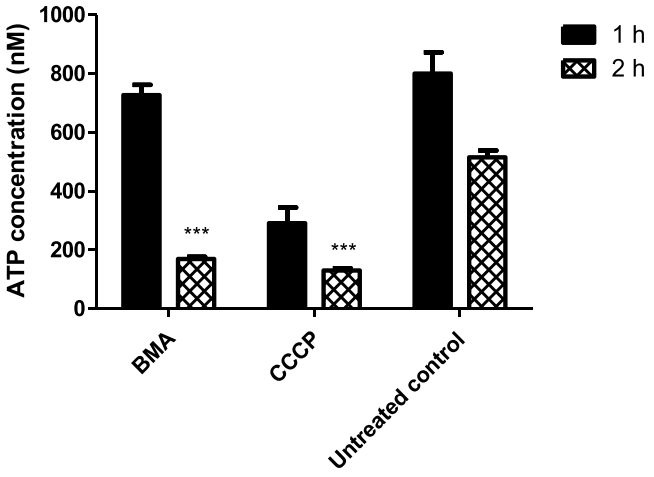

Figure 4. Evaluation of the ATP levels in trypomastigotes of *T. cruzi* after 1 and 2 h of treatment with **BMA**. CCCP was used as a positive control and the untreated parasites as a negative control. ***p < 0.001 relative to the negative control.

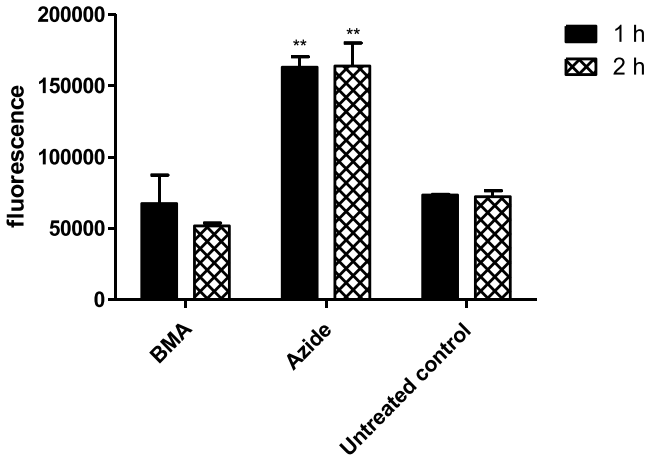

Figure 5. Evaluation of ROS in trypomastigotes after 1 and 2 h using H_2DCFDA (485 nm excitation and 535 nm emission). Untreated and sodium azide-treated parasites were the negative and positive controls, respectively. **p < 0.01 when compared to the control.

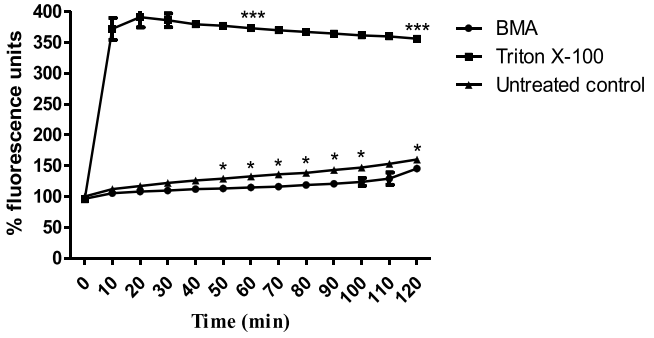

Figure 6. Calcium in trypomastigotes after 2 h of treatment with **BMA** using the Fluo-4 AM fluorophore (485 nm excitation and 535 nm emission). Untreated and 0.5% Triton X-100-treated parasites were used as negative and positive controls, respectively. *p < 0.05 and ***p < 0.001 relative to the negative control.

2.11. Mass Spectra Analysis of Trypomastigotes Treated with BMA. The protein mass spectral profile was evaluated using a Bruker MicroFlex MALDI-TOF/MS system. Trypomastigotes were treated with **BMA** (130 μM) and with the standard drug benznidazole (BZN, 40 μM) for 18 h. The data obtained with **BMA** and **BZN** showed considerable alterations in the mass spectra, demonstrating upregulation and downregulation of the main peaks. The mass spectra of untreated trypomastigotes were used as the control and demonstrated an increased number of proteins in the range of 2000−20,000 m/z (Figure 8).

3. DISCUSSION

Chagas disease affects mainly poor countries, and today, only two drugs are available; in Brazil, benznidazole is the only therapy. Considering the problems related to the COVID-19 pandemic that exacerbated the conditions for neglected tropical diseases, the introduction of innovative treatments is urgently needed.

Several natural compounds have been evaluated as antiparasitics, showing potent activities against these pathogenic microorganisms.[24,25] Particularly, marine metabolites have shown promising activities and have proved to be valuable sources of new drug candidates. Using bioactivity-guided fractionation, we discovered an antitrypanosomal indole alkaloid (**BMA**) in the marine coral *T. tagusensis* and investigated its antiparasitic effect and lethal mechanisms for the first time.

The alkaloid **BMA** demonstrated activity against the extracellular forms of the parasite, trypomastigotes, that was approximately 4-fold less active than benznidazole. Despite the importance of intracellular amastigotes for drug discovery studies, the Drugs for Neglected Disease Initiative (DND*i*) recommends that new candidates should also be effective against trypomastigotes, which are efficient for sustaining infections long after the clinical therapy. This fact makes trypomastigotes an important target for new hit compounds. Despite **BMA** being less effective against trypomastigotes, it showed good potency against intracellular amastigotes compared to benznidazole. Besides the potency, in vitro selectiveness (mammalian cytotoxicity/activity against amastigotes) has been one of the important topics for the criteria of hit compounds.[26] Don and Ioset[26] suggested that new hits against *T. cruzi* should present values of IC_{50} < 10 μM (amastigotes) and selectivity indexes >10. **BMA** showed no cytotoxicity in murine fibroblasts for the higher tested concentration. It is worth mentioning that cytotoxicity has been a limiting factor among promising natural compounds with anti-*T. cruzi* activity.[27−29] The isolated alkaloid (**BMA**) fulfilled the DND*i* criteria for a new hit compound and, additionally, showed a promising drug-like profile in an in silico medicinal chemistry platform.

In silico analysis for ADMET was performed using the SwissADME webserver. According to DND*i*, these studies are crucial for the selection of hit compounds, considering that poor pharmacokinetic and pharmacodynamic (PK/PD) profiles are the main reasons for candidate failures in clinical trials.[30]

Alkaloids are a highly structurally diverse group of compounds and are widely distributed in the marine environment, with many antiparasitic activities reported. The alkaloid renieramycin A, isolated from the sponge *Neopetrosia* sp., presented an IC_{50} of 0.35 μM against the protozoan parasite *Leishmania amazonensis*. Nortopsentin A, an imidazole alkaloid obtained from the sponge *Sponhosorites* sp., demonstrated antimalarial activity with an IC_{50} of 0.4 μM, resulting in

https://doi.org/10.1021/acsomega.2c03395
ACS Omega 2022, 7, 28561−28570

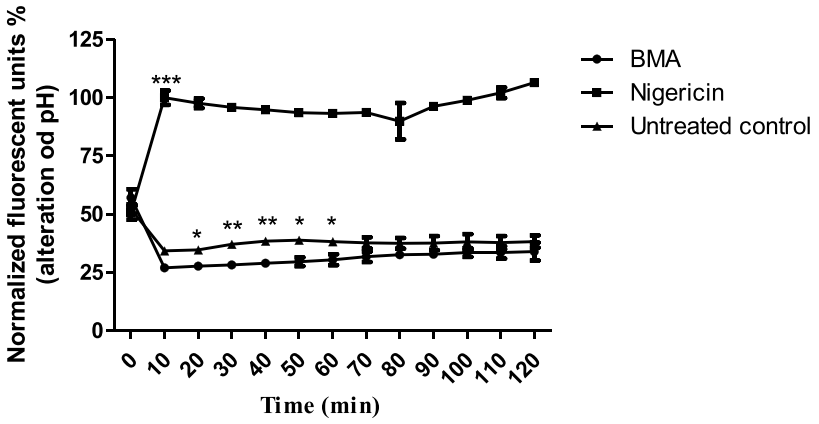

Figure 7. Alteration of the acidocalcisomes induced by **BMA** using the acridine orange dye (485 nm excitation and 535 nm emission). Nigericin was used as a positive control and the untreated parasites as a negative control. *$p < 0.05$; **$p < 0.01$, and ***$p < 0.001$ relative to the negative control.

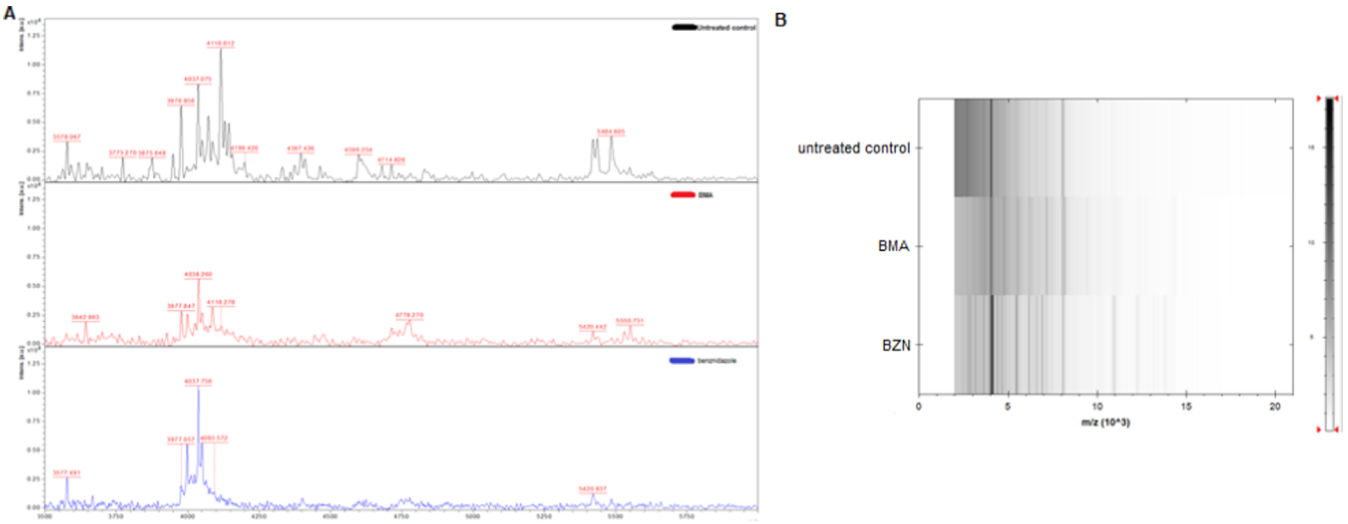

Figure 8. Evaluation of the mass spectra of trypomastigotes treated with **BMA** and the standard drug **BZN**. (A) A representative mass spectrum difference in the range of 3.000−6.000 *m*/*z*. Mass spectral data of **BMA**-treated trypomastigotes (red line) and those treated with **BZD** (blue lines). Parasites without any drugs were used as a negative control (black line). (B) A representative virtual gel (based on mass spectra in the range of 2.000−20.000 *m*/*z*). The absolute intensities and masses of the ions are shown on the *Y*- and *X*-axis, respectively. *m*/*z* represents the mass-to-charge ratio.

a selectivity of 14.[31] Psammaplysin F, isolated from *Hyatella* sp., showed an IC_{50} of 5.6 μM against *T. cruzi*, with a moderate selectivity index.

Indole alkaloids are the biggest class and comprise more than 4000 diversified members, with a bicyclic structure of a six-membered benzene ring linked to a five-membered nitrogen-containing pyrrole group. The marine bacterium *Bacillus pumilus*, obtained from *Antipathes* sp., yielded three indole alkaloids with IC_{50} values ranging from 19.4 to 26.9 μM.

In the early phases of drug discovery, the in silico analysis of ADMET and drug-like properties have been widely used to select promising hit compounds.[26,30] Considering the potential of **BMA** against *T. cruzi*, we investigated the adherence of the compound to drug-like properties using the SwissADME web platform. The predictions suggested that **BMA** has high gastrointestinal absorption and good oral bioavailability. Physicochemical analysis as Log *P*, which is defined as the relationship between the compound concentration in the organic phase and in the aqueous phase, demonstrated good values for Log *P* (1.73), as well as other parameters associated with the activity such as polarity (TPSA), molecular weight (size), and flexibility. Optimal values for Log *P* range from −0.7 to 5.0, and values higher than 5 will result in poor water solubility. Compound **BMA** presented a low molecular weight of 319 g/mol, which is in the optimal range between 150 and 500 g/mol.

For optimal flexibility, compounds should not exceed more than nine rotatable bonds,[32] and the predicted value of 1 for BMA was adequate for this model. The polarity of **BMA** resulted in a value of 74.48 Å, which is within the optimal range between 20 and 130 Å. Solubility (Log *S*) resulted in a value of −3.21; according to the ESOL model, the optimal value should not be higher than 6. Saturation, which represents the fraction of carbons in sp^3 hybridization, showed a value of 0.08 for **BMA**, but this value was not in agreement with the optimal value (≥0.25) described in the literature.

Pharmacokinetic parameters such as distribution are crucial for the target delivery of the drug in a living system. The compound **BMA** was not considered to be permeable through the blood−brain barrier, which is good for avoiding toxicity.[33]

https://doi.org/10.1021/acsomega.2c03395
ACS Omega 2022, 7, 28561−28570

However, **BMA** was not considered a *P*-glycoprotein (*P*-gp) substrate, which generally prevents xenobiotics from entering the brain and other barriers in mammals.[34,35]

Another parameter to be evaluated is the metabolization of molecules by cytochrome P450 (CYP). This superfamily of isoenzymes is responsible for drug elimination as a result of metabolic biotransformation. CYP has five main isoforms that interact with more than 90% of the approved drugs, i.e., CYP1A2, CYP2C19, CYP2C9, CYP2D6, and CYP3A4. When these CYPs are inhibited, chemical compounds can induce adverse effects and toxicity due to the accumulation in the blood or even in cells.[32,35] **BMA** was considered an inhibitor of only two CYPs, i.e., CYP1A2 and CYP2C19, thus showing a nonpromiscuous behavior.

This in silico analysis also provides access to five different rule-based filters. These filters projected by big pharmaceuticals aim to increase the excellence of their compound libraries. **BMA** did not violate any of the pharmaceutical filters tested, such as Lipinski, Ghose, Veber, Egan, and Muegge. This is an excellent parameter for the "go/no go" decisions in drug discovery programs.

The study of MoA is important to select promising candidates.[36] The cellular membrane is critical for parasite living, providing protection against the mammalian cell defense, conferring shapes, and being responsible for transporting nutrients and ions between the extracellular and intracellular environments.[37,38] The cellular membrane of *T. cruzi* is composed of glycoconjugates, which are often absent in mammals, making it an essential target to study. The activity of **BMA** in the plasma membrane of trypomastigotes was evaluated, and the compound did not alter the membrane of the parasite.

Mitochondria are responsible for energy production and many other processes such as calcium homeostasis and redox balance. In Trypanosomatidae, mitochondria are unique, making them an interesting target.[39,40] After a short incubation time, **BMA** produced significant depolarization ($\Delta\Psi_m$) in the parasite. This potential is generated by proton pumps and is essential for energy storage during oxidative phosphorylation.[40] Using a luminescence assay with luciferin, we also detected a significant reduction in the ATP levels of the parasite treated with **BMA**. This mitochondrial imbalance may have resulted in a respiratory chain collapse, affecting the ATP levels. ATP is a mediator of the bioenergetic system and is considered the most important energy source for cells.[39,41,42] These alterations in *T. cruzi* after treatment with **BMA** may have induced failures in oxidative phosphorylation, leading to metabolic damages, energy deficiency, and finally, death of the parasite.

ROS are generated by cells at minimal levels during ATP production in mitochondria. If not scavenged by the cell, these elevated ROS can accumulate, resulting in injury to DNA, proteins, and lipids, resulting in cell death. The ROS generated by mitochondria has a strong control, and the downregulation can result in autophagy and affects cell growth and differentiation.[43,44] Considering the mitochondrial imbalance and ATP variations, ROS levels were analyzed in trypomastigotes. **BMA** induced no variations in these levels for up to 2 h of treatment.

Besides their function in the energetic metabolism, mitochondria also contribute to calcium (Ca^{2+}) signaling and act as reservoirs. Intracellular calcium is essential for cell invasion and osmoregulation and also participates in the regulation of apoptosis.[45,46] Several Ca^{2+} channels were described in the *Trypanosoma* spp. plasma membrane in acidocalcisomes and in mitochondria. Ca^{2+} is also found in binding proteins present in the flagellum membrane.[46,47] In the present study, **BMA** induced a reduction in Ca^{2+} levels in trypomastigotes. This reduction can affect the parasite invasion and interfere with osmoregulation and homeostasis, leading to cell death.

Particularly, acidocalcisomes are electro-dense, membrane-bounded organelles present in all species. These acidic compartments are the major storage of phosphorus (poly P), calcium, and other cations. Acidocalcisomes are also responsible for the osmoregulation and maintenance of intracellular pH, which are sustained by two vacuolar proton pumps, pyrophosphatase and ATPase.[48−50] In our studies, the decreased fluorescence levels of the probe suggested the accumulation of acidocalcisomes. This fact may be ascribed to the intensification of the acidic environment, which might have influenced the Ca^{2+} storage, reducing its abundance in the cytoplasm of the parasite. The reduced levels of cytoplasmic calcium could be detrimental to cellular homeostasis, leading to the death of the parasite.

The metabolic alterations of the bioenergetic system of *T. cruzi* induced by **BMA** could also have compromised the metabolism of other macromolecules. Proteins are present in all living beings and participate in every cellular process, performing a range of functions in *T. cruzi*.[51] Proteins are required for DNA replication, evasion, and the virulence mechanism, modulating the host invasion. Moreover, proteins present in mitochondria are essential for most biosynthetic pathways.[52,53] In the present work, the mass spectra of *T. cruzi* proteins were obtained by the MicroFlex MALDI-TOF/MS, a system used for microorganism classification. Applying a machine learning model, the protein profile of **BMA**-treated parasites was compared to naïve parasites (untreated group) and those treated with the standard drug benznidazole. We observed significant mass spectral alterations in the treated parasites, demonstrating the imbalance of the protein metabolism, similar to those observed in the bioenergetic system. Van Oosten and co-workers (2020)[54] proposed this machine learning approach to select new antimicrobial compounds with novel mechanisms of action. Our data also revealed that **BMA** induced a different mass spectra profile from that obtained after the benznidazole treatment, the standard drug used for CD in Brazil. These data suggest that **BMA** might have a different lethal effect on *T. cruzi*, opening future possibilities of including **BMA** in combination therapy studies with BZN.

4. CONCLUSIONS

The marine environment is a valuable source of small molecules, offering compounds with promising activities against human diseases.[55] The antitrypanosomal activity of 6-bromo-2′-de-*N*-methylaplysinopsin (**BMA**) was presented for the first time against both forms of the parasite, leading to a lethal action due to the imbalance of the bioenergetic system and protein metabolism. Considering the lack of mammalian cytotoxicity, the elevated potency, selectivity, and the encouraging in silico drug-like profile, **BMA** should be used as a new scaffold in future drug design studies. The synthesis of new **BMA** derivatives could be useful in optimization studies against Chagas disease.

https://doi.org/10.1021/acsomega.2c03395
ACS Omega 2022, 7, 28561−28570

5. EXPERIMENTAL SECTION

5.1. Experimental Methods. Silica gel (230−400 mesh, Merck) and Sephadex LH-20 (Aldrich) were applied in column chromatography (CC), and silica gel 60 PF254 (Merck) was applied in thin layer chromatography (TLC). ^{1}H (500 and 600 MHz) and ^{13}C (125 and 150 MHz) NMR spectra were documented on a Varian INOVA 500 spectrometer with CD_3OD (Sigma-Aldrich) as the solvent and tetramethylsilane (TMS) as the internal standard. ESI-HRMS spectra were obtained with electrospray ionization in the positive ion mode on a Bruker Daltonics MicroTOF QII spectrometer. The equipment for high-performance liquid chromatography was a ultra performance liquid chromatography (UPLC) Prominence chromatograph (Shimadzu, Japan) supplied with LC-20AT gradient pumps and a ultraviolet (UV)−visible photodiode array detector (190−800 nm). MALDI-TOF/MS was performed on a Bruker MicroFlex spectrometer at a 20 kV accelerating voltage in the positive mode (500 laser shots). The signals were collected in a range between 2,000 and 20,000 m/z with the AutoXecute tool (Bruker Daltonics).[56]

5.2. Marine Coral. The coral *T. tagusensis* was collected in November 2021 in the Ilhabela region (São Paulo North Cost) at locations S 23°49′40.7″ W 045°24′44.7″ and S 23°46′26.9″ W 045°21′19.0″ at the Centro de Biologia Marinha da Universidade de São Paulo (USP, Brazil). The material was gathered by scuba diving at 2−10 m deep and using sterile plastic bags. The coral was immediately washed with filtered seawater to remove epifauna and identified. The colonies were separated from the sediment and then subjected to extraction procedures.

5.3. Extraction and Isolation. Colonies of *T. tagusensis* (1.8 kg) were macerated with MeOH (8 L). The solvent was reduced using an evaporator and an equal volume of H_2O was added. This solution was partitioned using *n*-hexane, EtOAc, and *n*-butanol. The activity against trypomastigotes of *T. cruzi* was identified in the EtOAc extract (3.75 g), and a sample (1.33 g) was applied to a Sephadex LH-20 (2.4 × 70 cm). The material was eluted with MeOH/EtOAc 1:1 (v/v), resulting in 90 fractions (10 mL each), which were assembled in six groups (A−F) after TLC analysis. After testing each obtained group, bioactivity was observed in group E (100 mg). Part of this material was analyzed by HPLC using an RP-ACE column (C_{18}, 25 × 0.46 cm^2, 5 μm) and eluted with MeOH/H_2O 15:85 to 100% MeOH for 28 min at 1.0 mL/min. This procedure afforded the compound 6-bromo-2′-de-*N*-methyl-aplysinopsin (**BMA**, 1.1 mg).

5.4. In Silico ADMET Studies. The drug-likeness profile of **BMA** was in silico analyzed using the SwissADME platform.[32] This tool is able to analyze not only multiple parameters such as absorption, distribution, metabolism, excretion, and toxicity (ADMET) but also physicochemical properties and drug-likeness with Big-Pharma filters.

5.5. Cells. *T. cruzi* (Y strain) was kept in LLC-MK2 (ATCC) using an RPMI-1640 medium containing 2% FBS at 37 °C in a 5% CO_2-humidified incubator. LLC-MK2 and NCTC (ATCC) cells were cultured at 37 °C in a 5% CO_2-humidified incubator in an M-199 medium supplemented with 10% FBS. Peritoneal macrophages were obtained from BALB/c mice and cultured at 37 °C.

5.6. Antitrypanosomal Activity. For the IC_{50} assay of **BMA**, trypomastigotes were added at 1 × 10^6 cells/well in 96-well microplates and treated (maximum concentration of 150 μM) for 24 h. Resazurin (0.011% in phosphate-buffered saline (PBS)) was used to detect parasite viability.[23] Untreated trypomastigotes were used as 100% viability. The analysis was performed at 570 nm using a spectrophotometer (FilterMax F5, Molecular Devices). Benznidazole was applied as the control drug.

The IC_{50} assay in the amastigote forms was obtained using peritoneal macrophages in 16-well plates (Thermo) at 1 × 10^5 cells/well. Macrophages were infected with trypomastigotes (1:10 ratio) for 2 h[23] and treated with **BMA** (2.03−65.0 μM) for 48 h. Giemsa was used for staining and the material was analyzed with a digital microscope (EVOS M500, Thermo). The infection index was obtained in 200 macrophages. Benznidazole was used as the standard.[57]

5.7. Determination of Mammalian Cytotoxicity. The 50% cytotoxic concentration was obtained in NCTC at 6 × 10^4 cells/well in 96-well microplates. The compound **BMA** (1.56−200 μM) was incubated for 48 h at 37 °C and the viability of the cells was determined by the MTT probe.[57] The optical density was determined at 570 nm using a FilterMax F5 (Molecular Devices).

5.8. Plasma Membrane Evaluation after BMA Treatment. The effect of **BMA** on the membrane of *T. cruzi* was assessed spectrofluorimetrically using the Sytox Green probe in a spectrofluorimeter.[24] Trypomastigotes were treated with a 1 μM fluorescent probe for 5 min in HBSS and glutamine. Then, **BMA** was added at 130 μM, and the fluorescence was observed for 2 h. Triton X-100 (0.5% v/v) was utilized as a control.[58]

5.9. Effects of BMA on Mitochondrial Potential ($\Delta\Psi_m$). The effects of **BMA** on $\Delta\Psi_m$ were observed with trypomastigotes (2 × 10^6 parasites/well) after treatment with **BMA** for 1 and 2 h. The fluorescent probe JC-1 dye (Molecular Probes) was included (10 μM) and trypomastigotes were kept for 20 min. The results were obtained in an Attune NxT flow cytometer (Thermo Fisher Scientific) at 488 nm (ex) and two emission filters of 530/574 nm. The ratio of 574 and 530 nm was used to obtain the mitochondrial membrane potential.[59] Carbonyl cyanide 3-chlorophenylhydrazone (CCCP) was used at 100 μM to obtain the maximum depolarization.

5.10. Measurement of ATP Levels of *T. cruzi*. The ATP levels of trypomastigotes were obtained after treatment with **BMA** (130 μM). The parasites were added at 2 × 10^6 parasites/well incubated for 1 and 2 h. Negative and positive controls were obtained with parasites without drugs and those incubated with CCCP (100 μM), respectively. The parasites were treated with 0.5% Triton X-100 (v/v) and incubated with a buffer (ATP Kit, Molecular Probes).[60] Luminescence intensity was obtained using a microplate luminometer (FilterMax F5 Multi-Mode, Molecular Devices).

5.11. Reactive Oxygen Species (ROS) Evaluation. The ROS levels were determined in trypomastigotes (2 × 10^6 parasites/well) after treatment with **BMA** (130 μM) for 1 and 2 h. Then, H_2DCFDA was added (5 μM), and the fluorescence was determined using a spectrofluorimeter (FilterMax F5) at 485 (ex) and 520 nm (em). The positive control was obtained with sodium azide (10 mM).[59]

5.12. Measurement of Intracellular Calcium Levels (Ca^{2+}) of *T. cruzi*. The calcium levels were studied in trypomastigotes (2 × 10^6 parasites/well) after treatment with **BMA** (130 μM). The parasites were pretreated with 5 μM Fluo-4 AM for 40 min at 37 °C and incubated with **BMA**. The

https://doi.org/10.1021/acsomega.2c03395
ACS Omega 2022, 7, 28561−28570

fluorescence was detected at 5, 20, 60, and 120 min using a spectrofluorimeter at 360 (ex) and 500 nm (em).[61,62] Triton X-100 (0.5% v/v) was used to obtain the maximum calcium levels.

5.13. Acidocalcisome Analysis of *T. cruzi*. The pH alterations of acidocalcisomes were studied in trypomastigotes of *T. cruzi* (2×10^6 parasites/well). The parasites were pretreated with acridine orange (4 μM) for 5 min and a basal reading was obtained. **BMA** was added at 130 μM. The fluorescence was monitored for 2 h using a spectrofluorimeter at 485 (ex) and 535 nm (em). Nigericin (4 μM) was used to obtain the maximum alkalinization levels.[63]

5.14. Mass Spectral Alterations of *T. cruzi*. Trypomastigotes (1×10^7 parasites/well) were treated with **BMA** (130 μM) and benznidazole (40 μM) for 18 h in the RPMI medium. After centrifugation, the pellet was resuspended in 300 μL of Milli-Q water, and 900 μL of 70% EtOH was added. Untreated parasites were used as the control.[55] The supernatant was applied (1 μL) on a MALDI slide, followed by 1 μL of cyano-4-hydroxy-cinnamic acid (CHCA).

5.15. Statistical Analysis. Sigmoidal dose−response curves were obtained by GraphPad Prism 5.0 software. Data were the mean ± standard error of two or three experiments.

■ ASSOCIATED CONTENT

Supporting Information

The Supporting Information is available free of charge at https://pubs.acs.org/doi/10.1021/acsomega.2c03395.

ESI-HRMS and NMR data (Figures S1−S7) with results of ESI-HRMS (positive mode); ^{1}H NMR; ^{13}C NMR; DEPT; DEPT 90°; HSQC NMR, and HMBC NMR spectrum of the alkaloid 6-bromo-2′-de-*N*-methylaplysinopsin (**BMA**) (PDF)

■ AUTHOR INFORMATION

Corresponding Authors

João Henrique G. Lago − *Centre of Natural Sciences and Humanities, Federal University of ABC (UFABC), Santo Andre, SP 09210-580, Brazil;* orcid.org/0000-0002-1193-8374; Email: joao.lago@ufabc.edu.br

Andre G. Tempone − *Centre for Parasitology and Mycology, Adolfo Lutz Institute, São Paulo, SP 01246-000, Brazil;* orcid.org/0000-0003-2559-7344; Email: andre.tempone@ial.sp.gov.br

Authors

Maiara M. Romanelli − *Centre for Parasitology and Mycology, Adolfo Lutz Institute, São Paulo, SP 01246-000, Brazil*

Maiara Amaral − *Centre for Parasitology and Mycology, Adolfo Lutz Institute, São Paulo, SP 01246-000, Brazil*

Fernanda Thevenard − *Centre of Natural Sciences and Humanities, Federal University of ABC (UFABC), Santo Andre, SP 09210-580, Brazil*

Lucas M. Santa Cruz − *Department of Organic Contaminants, Instituto Adolfo Lutz, São Paulo, SP 01246-000, Brazil*

Luis O. Regasini − *Department of Chemistry and Environmental Sciences, Institute of Biosciences, Humanities and Exact Sciences, Universidade Estadual Paulista, São Jose do Rio Preto, SP 15054-000, Brazil*

Alvaro E. Migotto − *Centre for Marine Biology, Universidade de São Paulo, São Paulo, SP 11600-000, Brazil*

Complete contact information is available at: https://pubs.acs.org/10.1021/acsomega.2c03395

Author Contributions

Author contributions were as follows: A.G.T. and J.H.G.L. designed the study; M.M.R. and A.E.M. collected and identified the coral; M.R. analyzed the data and isolated the natural product; M.M.R. and A.G.T. wrote the manuscript; J.H.G.L. performed the structural identification of **BMA**; L.O.R. and F.T. performed the NMR studies; L.M.S.C. performed the HPLC-HRMS studies; and A.G.T. organized the research and supported the study.

Funding

This work was supported by the São Paulo Research State Foundation (FAPESP, Projects 2021/04464-8, 2021/02789-7, and 2017/50333-7) and Conselho Nacional de Desenvolvimento Científico e Tecnológico (CNPq 405691/2021-1). The authors also acknowledge CAPES for the MR scholarship. This work was developed with members of the Research Network Natural Products against Neglected Diseases (ResNetNPND): http://www.uni-muenster.de/ResNetNPND/.

Notes

The authors declare no competing financial interest.

All procedures performed were previously approved by the Animal Care and Use Committee from Instituto Adolfo Lutz (Project 72J/2017) according to the National Academy of Science (NIH Publications No. 8023).

■ REFERENCES

(1) Moretti, N. S.; Mortara, R. A.; Schenkman, S. *Trypanosoma cruzi*. *Trends Parasitol.* **2020**, *36*, 404−405.

(2) Coura, J. R.; Viñas, P. A. Chagas disease: a new worldwide challenge. *Nature* **2010**, *465*, S6−S7.

(3) Jansen, A. M.; das Chagas Xavier, S. C.; Roque, A. L. R. *Trypanosoma cruzi* transmission in the wild and its most important reservoir hosts in Brazil. *Parasites Vectors* **2018**, *11*, No. 502.

(4) Rassi, A., Jr.; Rassi, A.; de Rezende, J. M. American trypanosomiasis (Chagas disease). *Infect. Dis. Clin. North Am.* **2012**, *26*, 275−291.

(5) WHO. World Health Organization. Integrating neglected tropical diseases into global health and development: fourth WHO report on neglected tropical diseases. Fourth WHO Report on Neglected Diseases, 2017. https://apps.who.int/iris/bitstream/handle/10665/255011/9789241565448-eng.pdf?sequence=1&isAllowed=y. (Accessed January 11, 2022).

(6) Zaidel, E. J.; Forsyth, C. J.; Novick, G.; Marcus, R.; Ribeiro, A. L. P.; Pinazo, M. J.; Morillo, C. A.; Echeverría, L. E.; Shikanai-Yasuda, M. A.; Buekens, P.; Perel, P.; Meymandi, S. K.; Ralston, K.; Pinto, F.; Sosa-Estani, S. COVID-19: Implications for People with Chagas Disease. *Global Heart* **2020**, *15*, No. 69.

(7) Bermudez, J.; Davies, C.; Simonazzi, A.; Real, J. P.; Palma, S. Current drug therapy and pharmaceutical challenges for Chagas disease. *Acta Trop.* **2016**, *156*, 1−16.

(8) Brum-Soares, L.; Cubides, J. C.; Burgos, I.; Monroy, C.; Castillo, L.; González, S.; Viñas, P. A.; Urrutia, P. P. High seroconversion rates in *Trypanosoma cruzi* chronic infection treated with benznidazole in people under 16 years in Guatemala. *Rev. Soc. Bras. Med. Trop.* **2016**, *49*, 721−727.

(9) Urbina, J. A.; Docampo, R. Specific chemotherapy of Chagas disease: controversies and advances. *Trends Parasitol.* **2003**, *19*, 495−501.

(10) Newman, D. J.; Cragg, G. M. Natural Products as Sources of New Drugs over the Nearly Four Decades from 01/1981 to 09/2019. *J. Nat. Prod.* **2020**, *83*, 770−803.

(11) Gul, W.; Hamann, M. T. Indole alkaloid marine natural products: an established source of cancer drug leads with considerable

promise for the control of parasitic, neurological and other diseases. *Life Sci.* **2005**, *78*, 442−453.
(12) Blunt, J. W.; Copp, B. R.; Keyzers, R. A.; Munro, M. H. G.; Prinsep, M. R. Marine natural products. *Nat. Prod. Rep.* **2016**, *33*, 382−431.
(13) Pereira, R. B.; Evdokimov, N. M.; Lefranc, F.; Valentão, P.; Kornienko, A.; Pereira, D. M.; Andrade, P. B.; Gomes, N. G. M. Marine-Derived Anticancer Agents: Clinical Benefits, Innovative Mechanisms, and New Targets. *Mar. Drugs* **2019**, *17*, No. 329.
(14) Scott, L. J. Brentuximab Vedotin: A Review in CD30-Positive Hodgkin Lymphoma. *Drugs* **2017**, *77*, 435−445.
(15) Álvarez-Bardón, M.; Pérez-Pertejo, Y.; Ordóñez, C.; Sepúlveda-Crespo, D.; Carballeira, N. M.; Tekwani, B. L.; Murugesan, S.; Martinez-Valladares, M.; García-Estrada, C.; Reguera, R. M.; Balaña-Fouce, R. Screening Marine Natural Products for New Drug Leads against Trypanosomatids and Malaria. *Mar. Drugs* **2020**, *18*, No. 187.
(16) Zanotti, A. A.; Gregoracci, G. B.; Capel, K. C. C.; Kitahara, M. V. Microbiome of the Southwestern Atlantic invasive scleractinian coral, *Tubastraea tagusensis*. *Anim. Microbiome* **2020**, *2*, No. 29.
(17) de Mello Carpes, R.; Fernandes, D. C.; Coelho, M. G. P.; Creed, J. C.; Fleury, B. G.; Garden, S. J.; Felzenszwalb, I. Anti-inflammatory potential of invasive sun corals (Scleractinia: *Tubastraea* spp.) from Brazil: alternative use for management? *J. Pharm. Pharmacol.* **2020**, *72*, 633−647.
(18) Lages, B. G.; Fleury, B. G.; Hovell, A. M. C.; Rezende, C. M.; Pinto, A. C.; Creed, J. C. Proximity to competitors changes secondary metabolites of non-indigenous cup corals, *Tubastraea* spp., in the southwest Atlantic. *Mar. Biol.* **2012**, *159*, 1551−1559.
(19) Sampaio, C. L. S.; Miranda, R. J.; Maia-Nogueira, R.; Nunes, J. A. C. C. New occurrences of the nonindigenous orange cup corals *Tubastraea coccinea* and *Tubastraea tagusensis* (Scleractinia: Dendrophylliidae) in Southwestern Atlantic. *Check List* **2012**, *8*, 528−530.
(20) Maia, L. F.; Ferreira, G. R.; Costa, R. C. C.; Lucas, N. C.; Teixeira, R. I.; Fleury, B. G.; Edwards, H. G. M.; de Oliveira, L. F. C. Raman spectroscopic study of antioxidant pigments from cup corals *Tubastraea* spp. *J. Phys. Chem. A* **2014**, *118*, 3429−3437.
(21) Djura, P.; Faulkner, D. J. Metabolites of the marine sponge *Dercitus* species. *J. Org. Chem.* **1980**, *45*, 735−773.
(22) Hu, J. F.; Schetz, J. A.; Kelly, M.; Peng, J. N.; Ang, K. K. H.; Flotow, H.; Leong, C. Y.; Ng, S. B.; Buss, A. D.; Wilkins, S. P.; Hamann, M. T. New antiinfective and human 5-HT2 receptor binding natural and semisynthetic compounds from the Jamaican sponge *Smenospongia aurea*. *J. Nat. Prod.* **2002**, *65*, 476−480.
(23) Guella, G.; Mancini, I.; Zibrowius, H.; Pietra, F. Aplysinopsin-type alkaloids from *Dendrophyllia* sp., a scleractinian coral of the family dendrophylliidae of the philippines, facile photochemical (Z/E) photoisomerization and thermal reversal. *Helv. Chim. Acta* **1989**, *72*, 1444−1450.
(24) Lima, M. L.; Romanelli, M. M.; Borborema, S. E. T.; Johns, D. M.; Migotto, A. E.; Lago, J. H. G.; Tempone, A. G. Antitrypanosomal activity of isololiolide isolated from the marine hydroid *Macrorhynchia philippina* (Cnidaria, Hydrozoa). *Bioorg. Chem.* **2019**, *89*, No. 103002.
(25) Martins, L. F.; Mesquita, J. T.; Pinto, E. G.; Costa-Silva, T. A.; Borborema, S. E.; Galisteo Junior, A. J.; Neves, B. J.; Andrade, C. H.; Shuhaib, Z. A.; Bennett, E. L.; Black, G. P.; Harper, P. M.; Evans, D. M.; Fituri, H. S.; Leyland, J. P.; Martin, C.; Roberts, T. D.; Thornhill, A. J.; Vale, S. A.; Howard-Jones, A.; Thomas, D. A.; Williams, H. L.; Overman, L. E.; Berlinck, R. G.; Murphy, P. J.; Tempone, A. G. Analogues of Marine Guanidine Alkaloids Are in Vitro Effective against *Trypanosoma cruzi* and Selectively Eliminate *Leishmania (L.) infantum* Intracellular Amastigotes. *J. Nat. Prod.* **2016**, *79*, 2202−2210.
(26) Don, R.; Ioset, J. R. Screening strategies to identify new chemical diversity for drug development to treat kinetoplastid infections. *Parasitology* **2014**, *141*, 140−146.
(27) Wright, A. D.; Goclik, E.; König, G. M.; Kaminsky, R. Lepadins D-F: antiplasmodial and antitrypanosomal decahydroquinoline derivatives from the tropical marine tunicate *Didemnum* sp. *J. Med. Chem.* **2002**, *45*, 3067−3072.
(28) Kossuga, M. H.; Nascimento, A. M.; Reimão, J. Q.; Tempone, A. G.; Taniwaki, N. N.; Veloso, K.; Ferreira, A. G.; Cavalcanti, B. C.; Pessoa, C.; Moraes, M. O.; Mayer, A. M.; Hajdu, E.; Berlinck, R. G. Antiparasitic, antineuroinflammatory, and cytotoxic polyketides from the marine sponge *Plakortis angulospiculatus* collected in Brazil. *J. Nat. Prod.* **2008**, *71*, 334−339.
(29) Regalado, E. L.; Tasdemir, D.; Kaiser, M.; Cachet, N.; Amade, P.; Thomas, O. P. Antiprotozoal steroidal saponins from the marine sponge *Pandaros acanthifolium*. *J. Nat. Prod.* **2010**, *73*, 1404−1410.
(30) Tuntland, T.; Ethell, B.; Kosaka, T.; Blasco, F.; Zang, R. X.; Jain, M.; Gould, T.; Hoffmaster, K. Implementation of pharmacokinetic and pharmacodynamic strategies in early research phases of drug discovery and development at Novartis Institute of Biomedical Research. *Front. Pharmacol.* **2014**, *5*, No. 174.
(31) Tempone, A. G.; Pieper, P.; Borborema, S. E. T.; Thevenard, F.; Lago, J. H. G.; Croft, S. L.; Anderson, E. A. Marine alkaloids as bioactive agents against protozoal neglected tropical diseases and malaria. *Nat. Prod. Rep.* **2021**, *38*, 2214−2235.
(32) Daina, A.; Michielin, O.; Zoete, V. SwissADME: a free web tool to evaluate pharmacokinetics, drug-likeness and medicinal chemistry friendliness of small molecules. *Sci. Rep.* **2017**, *7*, No. 42717.
(33) Monteiro-Neto, V.; de Souza, C. D.; Gonzaga, L. F.; da Silveira, B. C.; Sousa, N. C. F.; Pontes, J. P.; Santos, D. M.; Martins, W. C.; Pessoa, J. F. V.; Júnior, A. R. C.; Almeida, V. S. S.; de Oliveira, N. M. T.; de Araújo, T. S.; Maria-Ferreira, D.; Mendes, S. J. F.; Ferro, T. A. F.; Fernandes, E. S. Cuminaldehyde potentiates the antimicrobial actions of ciprofloxacin against *Staphylococcus aureus* and *Escherichia coli*. *PLoS One* **2020**, *15*, No. e0232987.
(34) Alavijeh, M. S.; Chishty, M.; Qaiser, M. Z.; Palmer, A. M. Drug metabolism and pharmacokinetics, the blood-brain barrier, and central nervous system drug discovery. *NeuroRx* **2005**, *2*, 554−571.
(35) Szakács, G.; Váradi, A.; Özvegy-Laczka, C.; Sarkadi, B. The role of ABC transporters in drug absorption, distribution, metabolism, excretion and toxicity (ADME-Tox). *Drug Discovery Today* **2008**, *3*, 379−393.
(36) Davis, R. L. Mechanism of Action and Target Identification: A Matter of Timing in Drug Discovery. *iScience* **2020**, *23*, No. 101487.
(37) Chen, R. R. Permeability issues in whole-cell bioprocesses and cellular membrane engineering. *Appl. Microbiol. Biotechnol.* **2007**, *74*, 730−738.
(38) Mucci, J.; Lantos, A. B.; Buscaglia, C. A.; Leguizamón, M. S.; Campetella, O. The *Trypanosoma cruzi* Surface, a Nanoscale Patchwork Quilt. *Trends Parasitol.* **2017**, *33*, 102−112.
(39) Menna-Barreto, R. F. S.; de Castro, S. L. The double-edged sword in pathogenic trypanosomatids: the pivotal role of mitochondria in oxidative stress and bioenergetics. *BioMed Res. Int.* **2014**, *2014*, 1−14.
(40) Smirlis, D.; Duszenko, M.; Ruiz, A. J.; Scoulica, E.; Bastien, P.; Fasel, N.; Soteriadou, K. Targeting essential pathways in trypanosomatids gives insights into protozoan mechanisms of cell death. *Parasites Vectors* **2010**, *3*, No. 107.
(41) Manzano, J. I.; Carvalho, L.; Pérez-Victoria, J. M.; Castanys, S.; Gamarro, F. Increased glycolytic ATP synthesis is associated with tafenoquine resistance in *Leishmania major*. *Antimicrob. Agents Chemother.* **2011**, *55*, 1045−1052.
(42) Rajendran, M.; Dane, E.; Conley, J.; Tantama, M. Imaging Adenosine Triphosphate (ATP). *Biol. Bull.* **2016**, *231*, 73−84.
(43) Reczek, C. R.; Chandel, N. S. ROS-dependent signal transduction. *Curr. Opin. Cell Biol.* **2015**, *33*, 8−13.
(44) Mittra, B.; Laranjeira-Silva, M. F.; de Menezes, J. P. B.; Jensen, J.; Michailowsky, V.; Andrews, N. W. A Trypanosomatid Iron Transporter that Regulates Mitochondrial Function Is Required for *Leishmania amazonensis* Virulence. *PLoS Pathog.* **2016**, *12*, No. e1005340.
(45) Ramakrishnan, S.; Docampo, R. Membrane Proteins in Trypanosomatids Involved in Ca^{2+} Homeostasis and Signaling. *Genes* **2018**, *9*, No. 304.

https://doi.org/10.1021/acsomega.2c03395
ACS Omega 2022, 7, 28561−28570

(46) Scarpelli, P. H.; Pecenin, M. F.; Garcia, C. R. S. Intracellular Ca^{2+} Signaling in Protozoan Parasites: An Overview with a Focus on Mitochondria. *Int. J. Mol. Sci.* **2021**, *22*, No. 469.
(47) Docampo, R. The origin and evolution of the acidocalcisome and its interactions with other organelles. *Mol. Biochem. Parasitol.* **2016**, *209*, 3−9.
(48) Docampo, R.; Moreno, S. N. J. Acidocalcisomes. *Cell Calcium* **2011**, *50*, 113−119.
(49) Docampo, R.; Huang, G. Calcium signaling in trypanosomatid parasites. *Cell Calcium* **2015**, *57*, 194−202.
(50) Lander, N.; Cordeiro, C.; Huang, G.; Docampo, R. Polyphosphate and acidocalcisomes. *Biochem. Soc. Trans.* **2016**, *44*, 1−6.
(51) Ferragut, F.; Acevedo, G. R.; Gómez, K. A. T Cell Specificity: A Great Challenge in Chagas Disease. *Front. Immunol.* **2021**, *12*, No. 674078.
(52) Maldonado, E.; Rojas, D. A.; Urbina, F.; Solari, A. The Use of Antioxidants as Potential Co-Adjuvants to Treat Chronic Chagas Disease. *Antioxidants* **2021**, *10*, No. 1022.
(53) de Castro Neto, A. L.; da Silveira, J. F.; Mortara, R. A. Comparative Analysis of Virulence Mechanisms of Trypanosomatids Pathogenic to Humans. *Front. Cell. Infect. Microbiol.* **2021**, *11*, No. 669079.
(54) van Oosten, L. N.; Klein, C. D. Machine Learning in Mass Spectrometry: A MALDI-TOF MS Approach to Phenotypic Antibacterial Screening. *J. Med. Chem.* **2020**, *63*, 8849−8856.
(55) Andrade, J. T.; Lima, W. G.; Sousa, J. F.; Saldanha, A. A.; De Sá, N. P.; Morais, F. B.; Silva, M. K. P.; Viana, G. H. R.; Johann, S.; Soares, A. C.; Araújo, L. A.; Fernandes, S. O. A.; Cardoso, V. N.; Ferreira, J. M. S. Design, synthesis, and biodistribution studies of new analogues of marine alkaloids: Potent *in vitro* and *in vivo* fungicidal agents against *Candida* spp. *Eur. J. Med. Chem.* **2021**, *210*, No. 113048.
(56) Mouri, O.; Morizot, G.; Van der Auwera, G.; Ravel, C.; Passet, M.; Chartrel, N.; Joly, I.; Thellier, M.; Jauréguiberry, S.; Caumes, E.; Mazier, D.; Marinach-Patrice, C.; Buffet, P. Easy identification of leishmania species by mass spectrometry. *PLoS Neglected Trop. Dis.* **2014**, *8*, No. e2841.
(57) Romanelli, M. M.; da Costa-Silva, T. A.; Cunha-Junior, E.; Ferreira, D. D.; Guerra, J. M.; Galisteo, A. J., Jr.; Pinto, E. G.; Barbosa, L. R. S.; Torres-Santos, E. C.; Tempone, A. G. Sertraline Delivered in Phosphatidylserine Liposomes Is Effective in an Experimental Model of Visceral Leishmaniasis. *Front. Cell. Infect. Microbiol.* **2019**, *9*, No. 353.
(58) Chicharro, C.; Granata, C.; Lozano, R.; Andreu, D.; Rivas, L. N-terminal fatty acid substitution increases the leishmanicidal activity of CA(1-7)M(2-9), a cecropin-melittin hybrid peptide. *Antimicrob. Agents Chemother.* **2001**, *45*, 2441−2449.
(59) Mukherjee, S. B.; Das, M.; Sudhandiran, G.; Shaha, C. Increase in cytosolic Ca^{2+} levels through the activation of non-selective cation channels induced by oxidative stress causes mitochondrial depolarization leading to apoptosis-like death in *Leishmania donovani* promastigotes. *J. Biol. Chem.* **2002**, *277*, 24717−24727.
(60) Dolai, S.; Yadav, R. K.; Pal, S.; Adak, S. Overexpression of mitochondrial *Leishmania major* ascorbate peroxidase enhances tolerance to oxidative stress-induced programmed cell death and protein damage. *Eukaryotic Cell* **2009**, *8*, 1721−1731.
(61) Sen, N.; Das, B. B.; Ganguly, A.; Mukherjee, T.; Bandyopadhyay, S.; Majumder, H. K. Camptothecin-induced imbalance in intracellular cation homeostasis regulates programmed cell death in unicellular hemoflagellate *Leishmania donovani*. *J. Biol. Chem.* **2004**, *279*, 52366−52375.
(62) Serrano-Martín, X.; García-Marchan, Y.; Fernandez, A.; Rodriguez, N.; Rojas, H.; Visbal, G.; Benaim, G. Amiodarone destabilizes intracellular Ca^{2+} homeostasis and biosynthesis of sterols in *Leishmania mexicana*. *Antimicrob. Agents Chemother.* **2009**, *53*, 1403−1410.
(63) Docampo, R.; Scott, D. A.; Vercesi, A. E.; Moreno, S. N. J. Intracellular Ca^{2+} storage in acidocalcisomes of *Trypanosoma cruzi*. *Biochem. J.* **1995**, *310*, 1005−1012.

https://doi.org/10.1021/acsomega.2c03395
ACS Omega 2022, 7, 28561−28570